DESIGN AND CONSTRUCTION OF AN INFRARED DETECTION SYSTEM FOR FOREST FIRES

By

RONALD KEITH JANTZ

Bachelor of Science

University of Wichita

Wichita, Kansas

1961

Submitted to the Faculty of the Graduate College
of the Oklahoma State University
in partial fulfillment of the requirements
for the Degree of
MASTER OF SCIENCE
May, 1969

DESIGN AND CONSTRUCTION OF AN INFRARED

DETECTION SYSTEM FOR FOREST FIRES

Thesis Approved:

William J. Lowe
Thesis Adviser

Arlo A. Schmidt

Edward E. Sturgeon

D. D. Durham
Dean of the Graduate College

ACKNOWLEDGMENTS

I want to thank Professor W. J. Leivo for suggesting the research problem and for his assistance and consultation. I express my appreciation to Professor A. R. Schmidt. The continuing interest in the work by Professor E. E. Sturgeon also requires my appreciation.

I am grateful for the fellowship granted to me by Harry Diamond Laboratories, Washington, D.C., that made this research possible. I wish to specifically thank those at Harry Diamond Laboratories who encouraged me to undertake this research: R. D. Hatcher, Fred Harris, Harold Gibson, Don Mary, R. G. Humphrey, and Frank Vrataric.

Most of all, I thank my devoted wife, Janice.

TABLE OF CONTENTS

LIST OF TABLES

LIST OF FIGURES

CHAPTER I

INTRODUCTION

The use of infrared sensors for military applications has been producing successful results for several years. Civilian uses for infrared sensors are now being rapidly explored and developed. The development of the techniques required to detect and measure infrared radiation experienced a gradual evolution. Barr (1) gives an account of the early development of the infrared spectrum. Other references (2,3,4) also review the military and civilian uses for infrared sensors. The application of infrared sensing to the detection and surveillance of forest fires is one of these uses.

The U.S. Forest Service, since 1961, has been conducting a forest fire detection research program at its Northern Forest Fire Laboratory, Missoula, Montana. Hirsch (5,6) has defined the extent of the fire detection problems and described the general performance requirements for operational fire detection systems. Wilson (7,8) has formulated the performance requirements for an airborne infrared scanner; results obtained with a prototype system are included. The infrared scanner produces a thermal map of the terrain under surveillance. The objective of the fire detection research program has been the development of a system capable of detecting both man-caused and lightning-caused fires day or night under all atmospheric conditions and in the wide variety of fuel and topographic conditions.

This thesis describes the design and construction of an infrared system to detect incipient forest fires. The system was built with the primary objective of investigating the various parameters and problems of forest fire detection. The system was built as simply as possible and the system performance would not be optimized.

The thesis reviews the characteristics of infrared radiation and the basic radiation laws. Factors determining the received signal at the aperture of an infrared system are examined and discussed. Target to background contrast, transmission through the atmosphere, and detector parameters all must be considered.

The infrared detection system which was designed and constructed is a tripod-mounted, battery-powered, portable instrument. The spectral pass band of the instrument, defined by the detector, is from 1 to 5 μ. The detector is a lead selenide detector operating at 295^{o}K. The main components of the system are the optical system, the detector and chopper, the preamplifier, and the power supply. A meter readout is obtained by using a portable ac voltmeter connected to the output of the system. The detection system can now be used as the basis for further study of the problems of forest fire detection. The objectives would be to develop techniques other than airborne mapping techniques.

CHAPTER II

THEORETICAL DISCUSSION

Characteristics of Infrared Radiation

The region of the electromagnetic spectrum where infrared radiation occurs is called the infrared spectrum. The unit of wavelength used in the infrared spectrum is the micron μ (1 micron = 10^{-4} cm). The spectrum has a lower limit of 0.72 μ and extends to approximately 1000 μ as shown in Figure 1. The wavelength λ is related to the frequency ν by

$$\lambda = \frac{C}{\nu} = \frac{1}{\nu'}$$

where C is the velocity of light ($C = 3 \times 10^{10}$ cm/sec.). The wavenumber ν' is the reciprocal of the wavelength λ. It is customary to use the actual frequency ν rather than the wave number ν' in discussions of blackbody radiation.

Any object whose temperature is above absolute zero radiates energy with much of it being radiated in the infrared spectrum. The emission is the result of accelerating charges within the object. The amount and spectral characteristics of the radiated infrared energy are dependent upon the absolute temperature of the object, its surface nature or emissivity, and its surface area.

Electromagnetic radiation may be classified by wavelength distribution as band spectra, line spectra, or continuous spectra or some combination of them. Band or line spectrum sources radiate strongly in

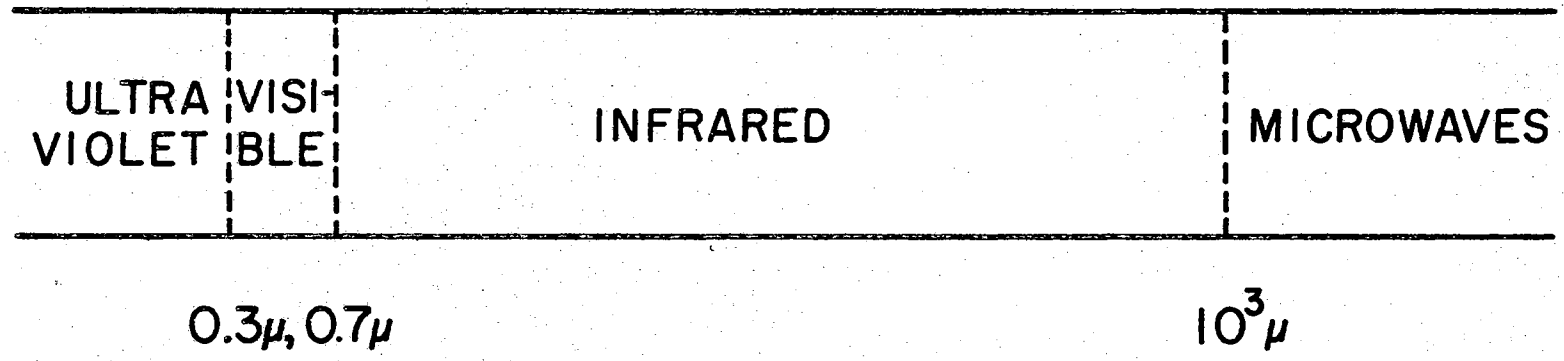

Figure 1. Location of the Infrared Spectrum in the Electromagnetic Spectrum

some narrow spectral intervals but in other wavelength intervals do not radiate at all. A plot of emission versus wavelength shows a series of emission bands or lines and the curve is discontinuous. Continuous sources emit radiation over a broad and continuous band of wavelengths. A plot of emission versus wavelength is a smooth curve usually having only one maximum. Each type of spectral source has found extensive use in basic research.

The thermal emission of solids is very difficult to explain by the use of electromagnetic theory. A thermodynamic approach has been used to explain the thermal emission of solids (9). The concept of an ideal radiator or "blackbody", fundamental to an understanding of the principles of infrared radiation, has evolved from this approach. The ideal radiator emits radiation over a broad and continuous band of wavelengths and thus is a continuous source. The following sections reveiw the basic radiation laws and the characteristics of the radiation for such ideal radiators. A discussion of the basic radiation laws and the characteristics of the radiation is covered by several authors (9,10,11, 12,13). The symbols used to describe radiometric quantities and their units are found in Table I.

The concept of a "blackbody" was postulated as an ideal absorber, absorbing all radiation incident upon it, and as an ideal radiator of radiation, emitting all radiation at the maximum possible, at all temperatures and for all wavelengths (13). Cavity-type blackbody sources, as used in the laboratory, approach the perfect blackbody. The blackbody is used as the standard for infrared work. The intensity of the radiation from such a cavity is a function of temperature only, and the radiation emitted approaches the blackbody continuous spectrum.

TABLE I

RADIOMETRIC QUANTITIES

Symbol	Name	Description		Units
A	Area	Projected area		cm^2
Ω	Solid Angle	----		sr
V	Volume	----		cm^2
U	Radiant energy	----		joule
u	Radiant energy density	Radiant energy per unit volume	$\frac{\partial U}{\partial V}$	joule cm^{-3}
P	Radiant Power	Rate of transfer of radiant energy	$\frac{\partial U}{\partial t}$	w
W	Radiant emittance	Radiant power per unit area emitted from a surface	$\frac{\partial P}{\partial A}$	w cm^{-2}
H	Irradiance	Radiant power per unit area incident upon a surface	$\frac{\partial P}{\partial A}$	w cm^{-2}
J	Radiant intensity	Radiant power per unit solid angle from a point source	$\frac{\partial P}{\partial \Omega}$	w sr^{-1}
N	Radiance	Radiant power per unit solid angle per unit projected area	$\frac{\partial^2 P}{\cos\theta \partial A \partial \Omega}$	w sr^{-1} cm^{-2}
P_λ	Spectral radiant power	Radiant power per unit wavelength interval	$\frac{\partial P}{\partial \lambda}$	w μ^{-1}
W_λ	Spectral radiant emittance	Radiant emittance per unit wavelength interval	$\frac{\partial W}{\partial \lambda}$	w $cm^{-2}\mu^{-1}$

TABLE I (Continued)

H_λ	Spectral irradiance	Irradiance per unit wavelength interval	$\frac{\partial H}{\partial \lambda}$	w cm^{-2} μ^{-1}
J_λ	Spectral radiant intensity	Radiant intensity per unit wavelength interval	$\frac{\partial J}{\partial \lambda}$	w sr^{-1} μ^{-1}
N_λ	Spectral radiance	Radiance per unit wavelength interval	$\frac{\partial N}{\partial \lambda}$	w sr^{-1} $cm^{-2}\mu^{-1}$

(After reference 11)

The radiation efficiency of a body is described by its emissivity ϵ. Emissivity is the ratio of the rate of radiant energy emission from a body, as a consequence of its temperature only, to the corresponding rate of emission from a blackbody at the same temperature (11). The emissivity ϵ of a blackbody is set equal to unity. A substance having a emissivity less than unity is termed a "graybody". The graybody radiate or absorb less radiant energy than a blackbody would at the same temperature.

Absorption, reflection, and transmission are the processes that account for all incident radiation on an object. The above terms must be equal to unity:

$$\alpha + \rho + \tau = 1$$

where the absorptance α is the ratio of the radiant energy absorbed by a body to the energy incident upon it. The radiant reflectance ρ is the ratio of the radiant energy reflected by a body to the energy incident upon it. The radiant transmittance τ is the ratio of the radiant energy transmitted through a body to the energy incident upon it. For an opaque material ($\tau = 0$) the expression is

$$\alpha + \rho = 1$$

then

$$\epsilon = 1 - \rho$$

where ϵ is the emissivity. The conditions characterized by a blackbody, a perfect absorber, are

$$\alpha = 1 \qquad \epsilon = 1 \qquad \rho = 0 \qquad \tau = 0.$$

Kirchoff's law states that the ratio of the radiant emittance W of any real body to the radiant emittance of a blackbody is given by

$$\frac{W}{\alpha} = W_{bb}$$

where α is the absorptance. For a blackbody $\alpha = 1$, and thus

$$\alpha = \epsilon$$

and

$$W = \epsilon W_{bb} = \alpha W_{bb}.$$

The above relation gives an expression for the radiant emittance for any source that is not a blackbody.

Planck's law represents the complete spectral distribution for a blackbody. Planck showed that it was necessary to assume that energy occurs only in discrete units of $h\nu$ and that the energy of a quantum of radiation is

$$E = h\nu$$

where h is Planck's constant ($h = 6.62 \times 10^{-27}$ erg sec). Planck's law states that the spectral radiant emittance W_λ of a blackbody at wavelength λ and at absolute temperature T is given by

$$W = \frac{C_1}{\lambda^5} (e^{C_2/\lambda T} - 1)^{-1}$$

where $C_1 = 3.74 \times 10^{-12}$ watt $cm^2 = 3.74 \times 10^4$ watts μ^4 cm^{-2} and

$C_2 = 1.438$ cm $^oK = 1.438 \times 10^4$ μ^oK.

The last values given for the constants are for use when the wavelength is expressed in μ. The spectral radiant emittance W_λ is expressed in watts cm^{-2} μ^{-1} of wavelength interval. The spectral radiant emittance versus wavelength plotted for a blackbody at various absolute temperatures is shown in Figure 2. A derivation of Planck's law can be obtained

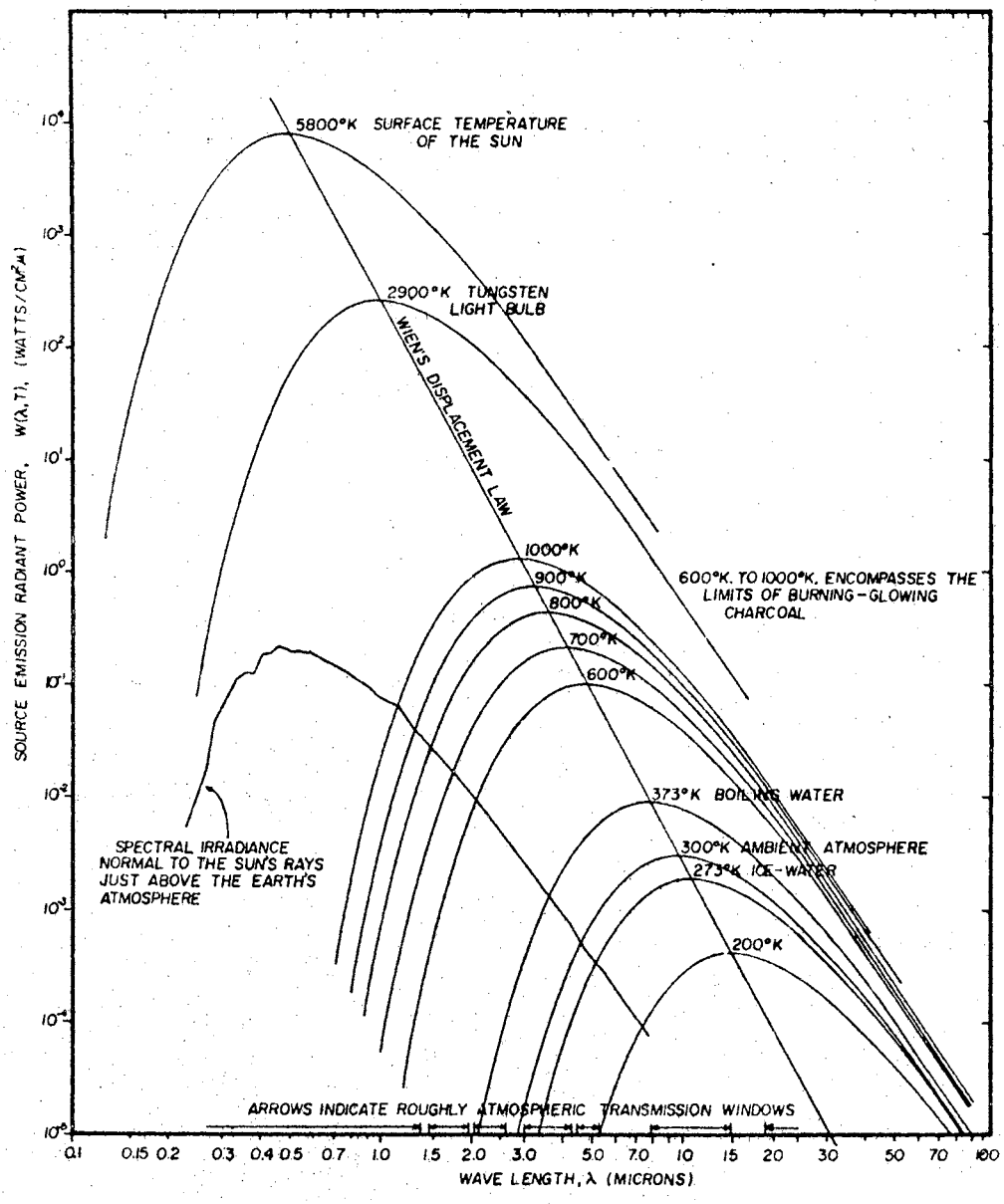

Figure 2. Spectral Power Curves Applicable to Forest Fire Surveillance. (After Wilson & Noste)

by considering the number of possible modes of oscillation for electromagnetic waves inside a cavity together with the average energy of each mode (10).

Integrating the Planck equation over all wavelengths yields the Stefan-Boltzmann law

$$W = \int_0^\infty W_\lambda \, d\lambda$$

$$W = \sigma T^4$$

where σ is the Stefan-Boltzmann constant ($\sigma = 5.67 \times 10^{-12}$ w cm^{-2}($^\circ$K)$^{-4}$). W is the total radiant emittance (w cm^{-2}) emitted by each square centimeter of surface area of a perfect blackbody at absolute temperature T ($^\circ$K). The expression of the Stefan-Boltzmann law for sources that are not a true blackbody is

$$W = \epsilon \sigma T^4$$

where ϵ is the emissivity.

The Wien Displacement law can be obtained from Planck's law by differentiating Planck's equation and setting the derivative equal to zero. The result obtained is

$$\lambda_{max} T = \text{constant} = 2897.9\mu \, (^\circ\text{K}).$$

Knowing the absolute temperature T of a blackbody, the Wein Displacement law tells where the peak of the radiation curve falls and the wavelength at which the maximum emittance occurs. A plot of the Wien Displacement law is shown in Figure 2.

The four basic radiation laws, Kirchoff's law, Planck's law, Stefan-Boltzmann law and Wein Displacement law have been reviewed.

Blackbody slide rules, using the basic radiation laws as the basis of their construction, have been built for rapid calculations of radiometric quantities. One such rule is the General Electric Radiation Calculator GEN-15C and is available from the General Electric Company. Application of the basic laws to a particular source require knowledge of the shape of the source, the surface area, and its temperature and emissivity.

A spherical source emits uniformly into 4π steradians, whereas an emitting plane surface is characterized by a cosine distribution. This cosine distribution is known as Lambert's law of cosines. A cavity-type blackbody source emits radiation from its aperture according to Lambert's law and is referred to as Lambertain source (11). The Lambertian surface has a constant radiance N which is the same in all directions. The radiant emittance W of a Lambertian surface is given by

$$W = \frac{P}{A} = \int N \cos\theta \, d\Omega$$

where P is the radiant power, A is the area, and Ω is the solid angle. The radiance N is defined as

$$N = \frac{\partial^2 P}{\cos\theta \, \partial A \partial \Omega} .$$

The differential solid angle defined in Figure 3 is

$$d\Omega = \frac{r^2 \sin\theta \, d\theta \, d\phi}{r^2} .$$

When the radiance of a surface at a point is $N = N(\theta,\varphi)$, the radiant emittance W at that point is

$$W = \iint N(\theta,\varphi) \cos\theta \sin\theta \, d\theta \, d\varphi$$

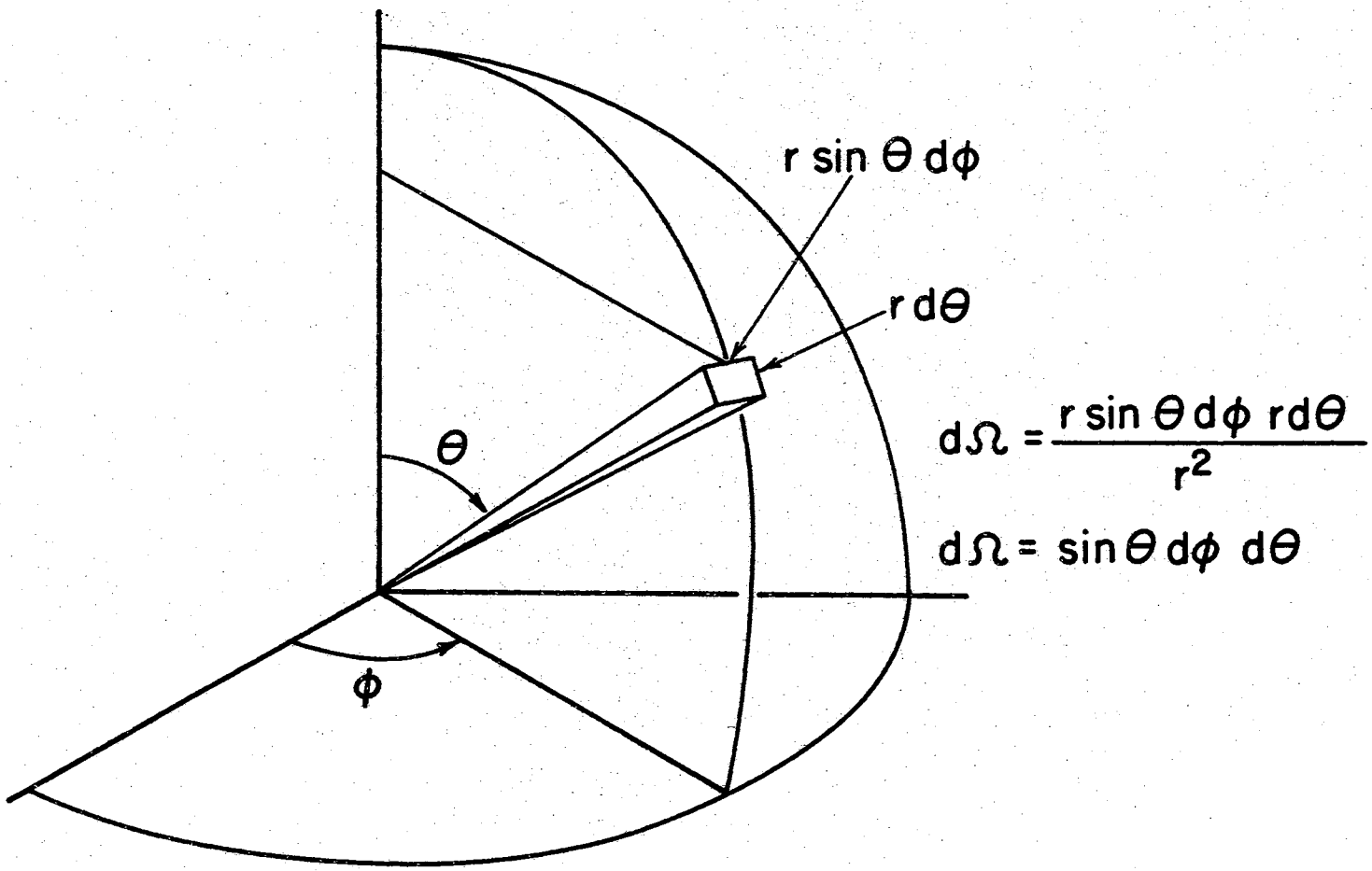

Figure 3. Differential Solid Angle

and the integration is carried out over the solid angle containing the radiation beam. If the beam is a perpendicular inverted circular cone of half angle α,

$$W = \int_0^{2\pi}\int_0^{\alpha} N(\theta,\varphi) \cos\theta \sin\theta \, d\theta \, d\varphi.$$

For a Lambertian surface N is constant and

$$W = 2\pi N \int_0^{\alpha} \cos\theta \sin\theta \, d\theta = \sin^2\alpha.$$

The radiant emittance from a Lambertian surface into a hemisphere ($\alpha = \frac{\pi}{2}$) is

$$W = \pi N.$$

Kruse, McGlauchlin, and McQuistan (9) have a discussion of emitting and absorbing characteristics of surfaces. Radiation emitted from real bodies can seldom be described or approximated by Lambert's cosine law. It is also difficult to characterize a real body by a single temperature and a simple area factor.

Infrared System Considerations

The application of infrared detection to the problem of reconnaissance and surveillance is of particular interest. An infrared system which depends upon the direct radiation from the target for detection is referred to as a passive infrared system. An active infrared system uses an artificial source to illuminate the target and the system detects the reradiated infrared energy. This discussion is concerned with the problems associated with a passive system. The primary objective of the system is the detection of a target against varying backgrounds

through an intervening atmosphere.

The design of an infrared system for reconnaissance and surveillance depends on many parameters but some are basic. The detection of the target ultimately depends on the contrast between the source radiation and the background radiation. The nature of the target, its characteristic radiation, emissivity, reflectivity, and range must be known. Background radiation is emitted by several sources and the nature of the radiation is important. The radiation emitted by the target and its background must pass through the atmosphere before it enters the infrared system. This may be a long passage through the earth's atmosphere, and the modification of the target and background radiation by absorption or scattering processes in the atmosphere must be taken into account. Consideration of these factors will indicate the specific wavelength region between which optimum system detectivity can be achieved.

Background and Target Radiation

Background radiation originates from natural sources which are of a terrestrial or celestial nature. Terrain background is due to all natural features of the terrain, trees, rocks, sand, earth and water. The terrain background may also include man-made objects such as buildings. A survey of the unclassified literature on terrain backgrounds is given by reference (14). The spectral characteristics of background radiation depend on the absolute temperature of the terrain, and the terrain characteristics as described by the emissivity and the reflectivity. Sky background, the background for all directions of view above the horizon, is formed by the atmosphere of the earth and by the sun,

moon, planets and stars beyond the atmosphere. Knowledge of the spectral distribution of the terrain or sky backgrounds is required to optimize the target-to-background contrast.

The spectral radiance N_λ of terrain is determined by emissivity, reflectivity, temperature of the terrain, and the effect of the intervening atmosphere. Reference (11) contains values for the above parameters. A mean temperature of approximately 300 ^{o}K may be used as the mean temperature for terrestrial surfaces. The surface temperature of the earth will depend upon the incident solar radiation, the nature of the terrain and the local weather conditions. Using the absolute temperature of 300^{o}K, the Wein Displacement law places the peak of the radiation curve near 10μ. This is the wavelength λ_{max}, or the wavelength at which the terrain emits its maximum radiation. The reflectance values for natural objects, at wavelengths shorter than 3μ, range from 0.03 for bare ground or ocean to 0.95 for fresh snow. Kruse, McGlauchlin, and McQuistan (9) suggest that for approximate calculations regarding the general level of background radiation, terrain can be assumed to be a gray body having emissivity of 0.35. The temperature of the terrain would be the temperature taken from a thermometer located in the terrain.

Measurements of the spectral radiance of nearby terrain (up to several hundred feet) show that it closely approximates a blackbody curve for the temperature of the terrain (11). When the temperature is 300^{o}K, the peak of the blackbody curve is at 10μ. A radiation slide rule calculation indicates that less than 0.2% of this energy is radiated below 4μ.

Radiation from terrain is the sum of the reflected sky radiation

plus the radiation emitted by a blackbody at the terrain temperature. The reflected sky radiation occurs below 4 μ and is from scattered or diffusely reflected sunlight. The daytime spectra of objects at ambient temperature show a minima around 3 to 4 μ . Measurements of the infrared spectral radiance from various objects and surfaces have been made (11). In the 10 μ region the spectral radiance of terrain follows changes in temperature. Near sundown the radiance falls rapidly and then slower during the night. After sunrise it rises to a maximum shortly after noon. Below 3 μ , the scattered radiation from the sun is dominant during the daytime. After sundown there is no infrared radiation from this source.

The effect of the atmosphere on the radiation from distant terrain has also been noted (11). The atmosphere absorbs radiation at certain wavelengths (discussed in the next section) and the radiation from distant terrain is altered at these wavelengths. The resulting spectral radiance measurements do not fit a single blackbody curve. At wavelengths where absorption takes place the observed radiance approximates a blackbody curve which has the same absolute temperature as the nearby terrain. At wavelengths where absorption does not take place the observed radiance fits a blackbody curve which has the same absolute temperature as the distant terrain. The effect of atmospheric absorption on the design of infrared systems is illustrated by this example.

Sky background radiation is caused by the scattering of the solar radiation and by the thermal emission of radiation from the molecules in the atmosphere. The scattered radiation being scattered from the molecules, particles and water droplets in the atmosphere is particularly affected by cloud distribution. The solar scattering region is the

region of the spectrum below 3 μ, and the thermal emission region beyond 4 μ. Solar scattering can be represented by reflection from a sunlit cloud. An upper limit of sky radiance assumes that all the sun's radiation is uniformly scattered toward the earth so the sky has a uniform brightness. Under this condition the radiance occurs at 0.5 μ. A plot of the spectral irradiance for the sun's rays is given in Figure 2. The figure also shows the spectral distribution of the sun observed through the atmosphere as approximated by a blackbody at 5800°K. The thermal emission region can be represented by a 300°K blackbody (6).

Infrared Transmission Through the Atmosphere

Infrared radiation transmitted through the earth's atmosphere is attenuated at certain wavelengths and the effect on the performance of an infrared system must be considered. The radiation is attenuated because of absorption due to the gases of the atmosphere. Radiation may also be scattered by particles suspended in the path through the atmosphere.

Infrared radiation can penetrate smoke and atmospheric haze more effectively than visible light because of its longer wavelength relative to the particle size in the scattered haze. Transmission of infrared through fog and clouds is little better than visible light for water vapor particle size renders them opaque. The optical properties of the atmosphere, the theory of molecular absorption, and the theory of scattering by the atmosphere (Rayleigh scattering and Mie scattering) are discussed by Kruse, McGlauchlin and McQuistan (9). The gases present in the atmosphere in the greatest abundance are nitrogen, oxygen, water vapor, carbon dioxide, methane, nitrous oxide, carbon monoxide,

and ozone. The gases oxygen and nitrogen are the gases with the highest concentration, but they do not exhibit any molecular absorption bands. The most important gases at sea level and up to 40,000 ft. which have absorption bands are water vapor and carbon dioxide. Water vapor has absorption bands at 1.1 μ, 1.38 μ, 1.87 μ, 2.7 μ and 6 μ. Carbon dioxide bands are located at 2.7 μ, 4.3 μ and 14.5 μ (9). The atmospheric transmission curves up to 5.5 μ are shown in Figure 4 and Figure 5 (10). The figures show the water vapor and carbon dioxide absorption bands. The atmosphere is essentially opaque to infrared radiation in these absorption bands. The transmission curves also show regions of relatively high transmission between the absorption bands. These regions are referred to as "atmospheric windows." The spectral limits are 1.5-1.8 μ, 2-2.6 μ, 3-4.2 μ, 4.5-5.3 μ, and 8-14 μ. The term "atmospheric window" is a qualitative term for the windows will broaden or narrow as a function of altitude, barometric pressure, and the concentration of water vapor and carbon dioxide in the atmosphere. Transmission through the windows is correspondingly affected. The consideration given these regions of atmospheric transmission greatly affect the spectral requirements of components used in infrared systems.

Infrared Detectors

The detection of infrared radiation may be accomplished by any one of three basic interactions of the radiation with the surface of a semiconductor. The three forms of interaction all give rise to photoeffects and can be referred to as the external photoeffect, the internal photoeffect and the thermal effect.

The external photoeffect is more commonly called the photoelectric

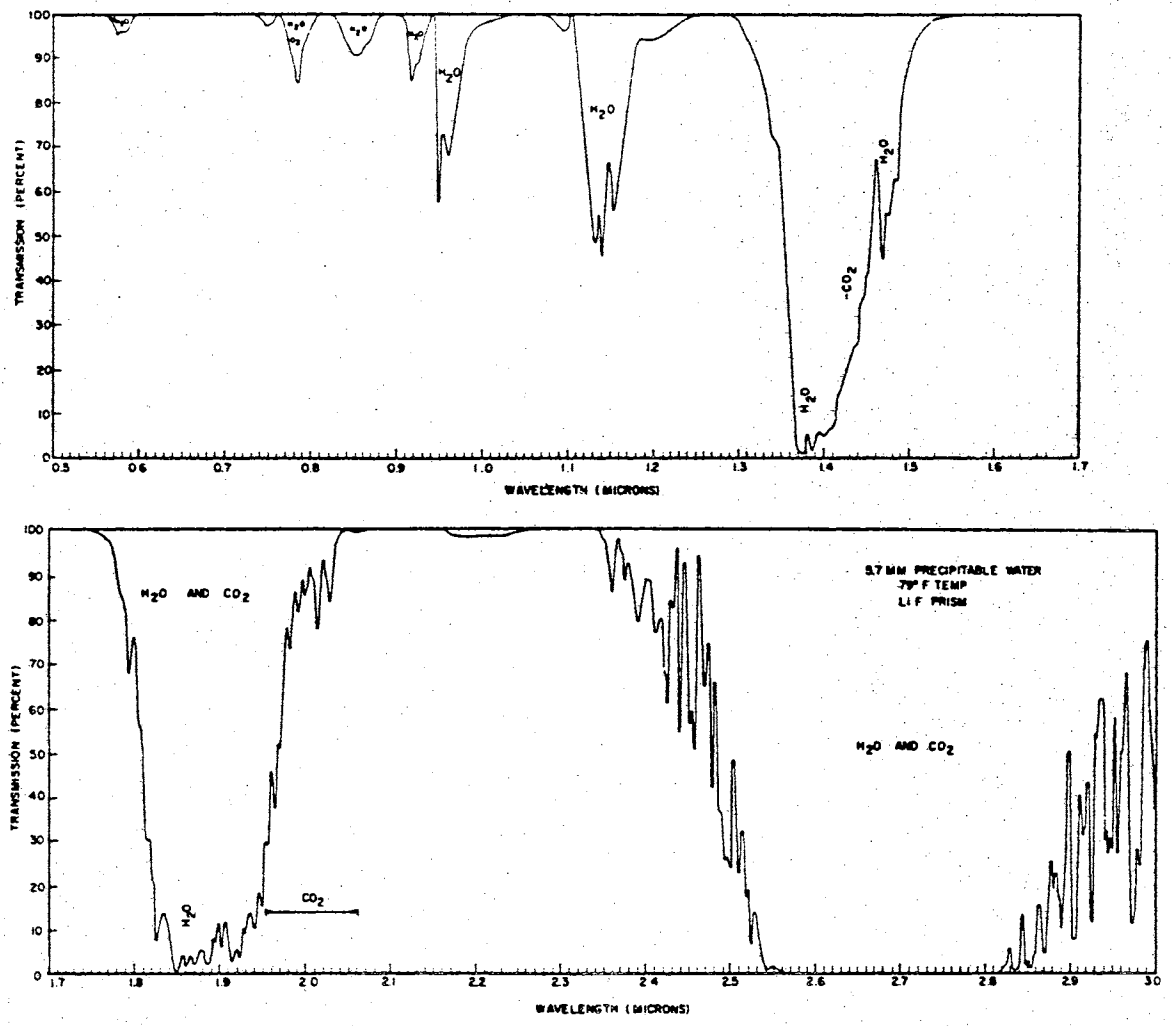

Figure 4. Atmospheric Transmission Over a 0.3 Km Sea Level Path in the 0.5-3.0μ Region.(After Yates and Taylor)

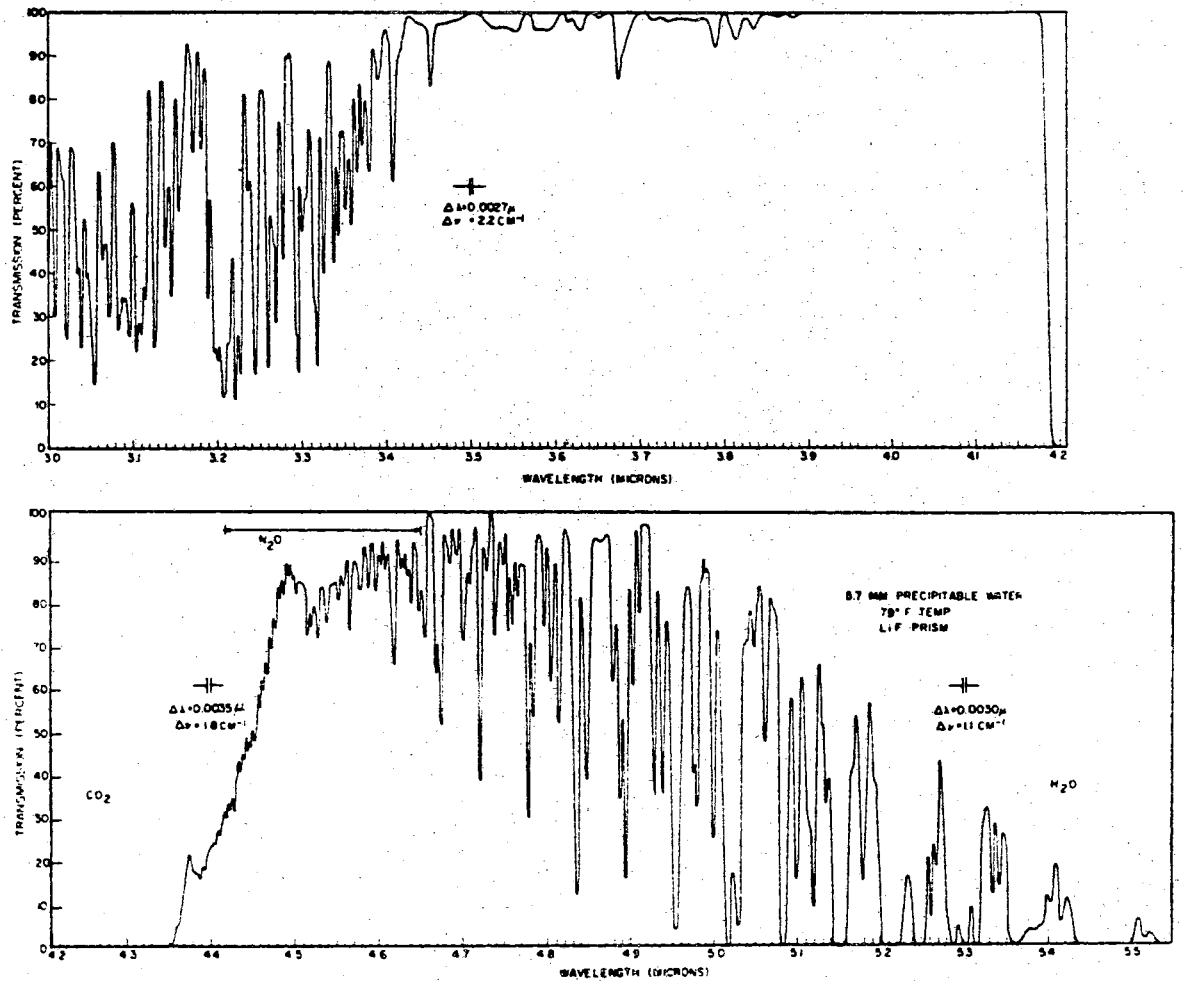

Figure 5. Atmospheric Transmission Over a 0.3 Km Sea Level Path in the 3.0-5.5μ Region. (After Yates and Taylor)

effect. It occurs when the incident photon interacts with the material with an energy greater than the threshold energy or the minimum energy required to free an electron from the material. The internal photoeffect occurs when a photon having energy greater than a minimum required by the material interacts with the material to produce a free electron, a free hole, or both. Internal photoeffects include photoconductivity, photovoltaic effect, and photoelectromagnetic effect. Detectors based upon either the external or internal photoeffects are called photodetectors.

The thermal effect results from the interaction of radiation with the material, heating the material as the energy is absorbed, causing a temperature rise in the material. The resistivity of the material is a function of the temperature. Measuring a change in the resistivity results in detection of the radiation.

The detection mechanisms thus classify detectors according to two types; thermal detectors and photodetectors. Thermal detectors have responsive elements sensitive to changes in temperature due to changes in incident power. They respond equally well to radiant energy of all wavelengths, or have a flat response. The response time, however, is measured in milliseconds. Examples of thermal detectors are metal and thermistor bolometers, thermocouples, and Golay cells (9). Photodetectors have responsive elements which are sensitivie to fluctuations in the number of incident photons. Photodetectors are responsive only over a certain spectral region, responding only to those photons of sufficiently short wavelengths. Their response is also proportional to the rate at which photons are absorbed at a given wavelength. Assuming equal amounts of incident power at any particular wavelength, the re-

sponse usually decreases as the wavelength decreases below the wavelength λc corresponding to minimum energy. The response time of photodetectors is measured in microseconds.

Photodetectors are classified according to the effect used to detect the fluctuations in incident photons. The common types are photovoltaic detectors, photoconductive detectors and photoelectromagnetic detectors. Any change in the photon flux incident upon a photovoltaic detector results in fluctuations in the voltage generated by the detector. The photovoltaic detector has the advantage that it requires no bias voltage. Photoelectromagnetic detectors place the responsive element in a magnetic field. Photons absorbed at the surface of the element generate charge carriers which diffuse into the bulk and are seperated by the magnetic field. This separation of charge produces an output voltage which fluctuates according to the fluctuations in the number of incident photons. No bias voltage is required. Any change in the number of photons incident upon a photoconductive detector results in fluctuations in the number of free charge carriers in the semiconductive material. The electrical conductivity of the responsive element is inversely proportional to the photon flux. Detection of the radiation is accomplished by monitoring the changes in the conductivity.

The detection mechanisms of infrared detectors are discussed throughly by reference (9) and reference (10). Reference (9) is most complete, presenting a discussion of the mathematical theory of the most important infrared detection mechanisms. The sources of detector noise, thermal noise, 1/f noise, generation recombination noise, and shot noise are covered. The ideal photon detector or "Blip" detector has no internally generated noise and is capable of counting every photon of

wavelength shorter than the cutoff wavelength λc which reaches the detector. The photon noise limit of the "Blip" detector is discussed by reference (9).

Detector Parameters

The selection of an infrared detector must be based upon parameters that adequately describe the detectors general characteristics and the nature of its response to radiation. The parameters used must also allow comparison of the performance of a particular detector to detectors of different types. A definitive report setting the standards for infrared detection measurements and the parameters for describing their performance is given by reference (16). The standard report on a particular detector includes a description of a detector, the conditions of measurement, a diagram of the input circuit to the preamplifier, and the data on the test results. Data on commercially available infrared detectors of all types is given by reference (11).

Various parameters must be specified in order to describe the performance of detectors. These parameters include such things as the responsive area, modulation frequency, spectral character of the radiant power, bias voltage level, and the electrical bandwidth of the measuring equipment. Figures of merit have been defined which take into account these parameters and allow two independent measurements of a detector's performance to be compared. The figures of merit are responsivity R, noise equivalent power NEP, normalized detectivity, and time constant τ. These are the figures of merit most commonly used; a complete list of detector parameters are defined and placed in a table by reference (11).

The responsivity R is defined as the ratio of the rms signal vol-

tage Vs at the fundamental radiation signal frequency to the rms radiation signal power Ps at the same frequency. The ratio is

$$R = \frac{Vs,\ rms}{Ps,\ rms} \quad \text{volts rms/watts rms.}$$

The responsivity of a particular detector is governed by the parameters such as the spectrum of the incident radiation, the frequency f used to chop the radiation, the operating temperature of the detector, and the bias voltage b. The responsivity written as a function of these parameters is

$$R = R(b,\ f, \lambda)$$

where λ denotes the spectral dependence.

The noise equivalent power NEP is defined as the minimum rms value of the fundamental frequency component of the radiant signal power P_s falling on the detector which will give rise to an rms signal voltage Vs equal to the rms noise voltage Vn from the detector. NEP is

$$NEP = Ps,rms\ (Vs,rms/Vn,rms)^{-1} \quad \text{watt}$$

or

$$NEP = Vn,rms/R.$$

NEP is a function of the various operating parameters of the cell. The signal voltage Vs varies with the bias voltage, chopping frequency, and responsive area. The noise voltage Vn varies with the bias, chopping frequency, responsive area, and electrical bandwidth. The radiant signal power Ps varies with wavelength and responsive area. A blackbody source of absolute temperature $500^{\circ}K$ is the standard used in test measurements. The results of the test express NEP as

NEP (500°K, 840,15).

The 840 refers to the chopping frequency f and the 15 refers to a 15 Hz bandpass.

It must be remembered that NEP cannot be used to compare different detectors unless the value of NEP is adjusted to account for possible differences in the responsive areas or the differences which might exist in the measurement procedure. A figure of merit has been defined which does eliminate the problem of area and bandwidth dependence. The term commonly used for the comparison of detectors is the normalized detectivity D^*. The normalized detectivity D^* is given by

$$D^* = \frac{(A\ \Delta f)1/2}{NEP} \quad \text{cm (Hz)}^{1/2}\ \text{watt}^{-1}$$

In order to designate the test conditions, D^* is written as

$$D^* (\lambda,f) = (A\ \ \Delta f)^{1/2}/NEP\ (\lambda, f, \Delta f)$$

$$D^* (500^\circ K, 840) = (A\ \ \Delta f)^{1/2}/NEP\ (500^\circ K, 840, 15)$$

where 840 is the chopping frequency f and 15 is the 15_{Hz} bandpass.

The time constant is a measure of the speed of response of a detector. The time constant indicates what range of frequency in the fluctuation of signal radiation power the responsive element can follow. The responsivity can be measured as a function of relative response versus frequency. This is accomplished by varying the chopping rate of the chopper. The detector time constant is estimated from this curve. The time constant τ is

$$\tau = 1/2\pi f_c$$

where f_c is the chopping frequency at which the responsivity has fallen

to 0.707 of its maximum value.

System Sensitivity

The selection of a detector for an infrared system will depend on the function of the system. If the function of the system is to obtain a radiometric measurement of a source, the detector must cover the range of expected radiation with a minimum variation in spectral sensitivity. Thermal detectors with their flat response are used to make radiometric measurements. If the function of the system is simply the detection of the source or target, a detector is selected on the basis of its response over the spectral region in which the best possible source-to-background contrast can be obtained. Photoconductive or photovoltaic detectors possessing high values of D^* over a limited spectral region are generally used. The high values of D^* usually require cooling of the responsive element. The term sensitivity has reference to the signal to noise ratio of the infrared system. The signal due to the target radiation must exceed the signal due to the background radiation by an amount which is equal to, or greater than, the detector or system noise. The detector is selected according to the function of the system and is the main factor determining the sensitivity of the infrared system.

A general approach to the calculation of the sensitivity of an infrared system will be outlined. Larmore describes a range equation for passive infrared devices (17). Other range equations and detection criteria are discussed in references (11,12,18,19). The determination of the maximum range of an infrared system requires a detailed analysis of the spectral radiance properties of the target, the absorption in the

intervening atmosphere, and the response of the detector. These factors have all been previously discussed. A range equation containing these factors has been formulated, but its solution is not a simple task.

At the aperture of the infrared system, located at a distance R from the source, the spectral irradiance H_λ is

$$H_\lambda = \frac{J_\lambda \ \tau_{a(\lambda)}}{R^2}$$

where J_λ is the spectral radiant intensity of the source, and $\tau_a(\lambda)$ is the spectral transmittance of the intervening atmosphere between the target and system aperture. Some real sources can be approximated by the Lambert cosine law. This assumes the source radiates from a flat surface and is close to a blackbody. The spectral radiant intensity J_λ in the direction of the normal to the radiating surface is

$$J_\lambda = N_\lambda A$$

where A is the projection of the target area and N_λ is the spectral radiance. Using the result for the spectral radiance of a Lambertian surface derived earlier for this case,

$$N_\lambda = \frac{1}{\pi} W_\lambda$$

and

$$J_\lambda = \frac{1}{\pi} W_\lambda \ A$$

Now the spectral irradiance at the aperture is

$$H_\lambda = \frac{W_\lambda \ A \ \tau_{a(\lambda)}}{\pi \ R^2} .$$

W_λ is the spectral emittance of the target as given by the spectral emittance of a blackbody at an absolute temperature of T^o Kelvin modi-

fied by the emissivity ε of the target.

The spectral transmission factor $\tau_o(\lambda)$, determined by the optics of the system, is given by

$$\tau_o(\lambda) = A_o\, t_o.$$

A_o is the effective aperture area in cm^2, and t_o is the transmission of the optical system. $\tau_o(\lambda)$ varies between zero and one.

In order to allow for the wavelength dependent response characteristics of the detector, the relative spectral response of the detector $\Sigma(\lambda)$ is used. The effective radiation at wavelength λ falling on the detector becomes

$$S_\lambda = H_\lambda\, \tau_o(\lambda)\, \Sigma(\lambda)$$

The total signal power available to the detection system is

$$S = \int_o^\infty \frac{W_\lambda\, A\, \tau_o(\lambda)\, \tau_a(\lambda)\, \Sigma(\lambda)\, d\lambda}{\pi R^2}$$

The detection of a target with signal power S depends upon the signal to noise ratio S/N which can be tolerated and the value of the noise N introducted into the system by the background radiation, the electronics, or the detector itself. The signal to noise ratio is

$$\frac{S}{N} = \frac{S}{NEP}$$

where NEP was defined as

$$NEP = \frac{(A_d \Delta f)^{1/2}}{D^*} .$$

Thus, S/N can be written as

$$S/N = \frac{A}{\pi R^2 NEP} \int_0^\infty W_\lambda \tau_a(\lambda) \tau_o(\lambda) \Sigma(\lambda) d\lambda$$

This equation can be solved directly for the range R only for special cases where the atmospheric transmittance $\tau_a(\lambda)$ is independent of R.

$\tau_a(\lambda)$ is independent of R only at higher altitudes. For this special case the range is

$$R = \left[\frac{A}{\pi NEP\ S/N} \int_0^\infty W_\lambda \tau_a(\lambda) \tau_o(\lambda) \Sigma(\lambda) d\lambda \right]^{1/2}$$

At altitudes where $\tau_a(\lambda)$ is a function of path length R, graphical or numerical methods must be used. Reference (14) discusses this graphical solution method.

CHAPTER III

INFRARED SYSTEM DESIGN AND CONSTRUCTION

Preliminary Design Considerations

The choice of components for an infrared system is determined by the function of the instrument and the kind of information desired. A passive infrared system was discussed as having its primary objective the detection of a target against varying backgrounds through an intervening atmosphere. In order to construct such a system, all the factors discussed in the last chapter must be considered.

The problem proposed was to build an infrared system capable of detecting small fires in order to study the problems of fire detection. The infrared system was built under the assumption that the materials used would be inexpensive and readily available. The instrument must be rugged enough to be taken into the field and have its own power supply. The construction of the system would provide information on forest fire detection problems and through its construction the author would gain an understanding of infrared systems.

The basic function of the proposed infrared system would be the detection of a small fire against a forest background. A search capability would be required to the extent that the system could be aimed in the general direction of the target and detection would occur. The field of view of the instrument was to be as large as cost and materials would permit. Sensitivity of the instrument would be governed by

the components selected. The particular detector selected and the optical system used are the most critical factors determining sensitivity. The spectral characteristics of the target, the background, and the atmospheric transmission dictate the selection of the detector.

Wilson (8) discussed the spectral criteria required for the detection of forest fires by infrared systems. Glowing, burning fuels associated with applications in forest fire surveillance closely approximate the ideal blackbody radiation curves (Figure 2). The limits of 600°K to 1000°K are the absolute temperature limits used to define glowing and burning fuels. Simulated fire targets described by Wilson and Noste (7), consist of a 14 inch diameter bucket filled with 10 pounds of charcoal. The temperatures of the burning charcoal measured with a thermocouple, ranged from 700°F to 1190°F (643°K to 913°K) and averaged 892°F (750°K). The radiometer measurement of 895°F (752°K) agreed closely. The source emission was found to be steady between one-half hour and 5 hours after ignition. The radiant energy from this source was measured as a function of the vertical angle referenced to the normal to the source. The energy distribution showed the source closely approximates a Lambertian source.

The mean temperature of the target is 750°K, with lower and upper limits of 600°K and 1000°K respectively. A calculation using the Wien Displacement will give the wavelength λ_{max} at which the maximum radiation will occur. The mean temperature of 750°K has λ_{max} at 3.85 μ. The lower and upper temperature limits of 600°K and 1000°K have λ_{max} occuring at 4.80 μ and 2.89 μ. Glowing and burning fuels emit their maximum radiation between 3 μ and 5 μ.

The effect of background radiation superimposed upon the source

radiation is the introduction of unwanted noise into the infrared system. The sources of background radiation were discussed earlier. The temperature of terrain was said to have a mean temperature of 300°K and a maximum radiant energy is emitted near 10μ. The emissivity of terrain was taken to be 0.35. The spectral radiance of terrain results from thermal emission from the terrain and radiation reflected from the ground as well as scattered and emitted radiation coming from the atmosphere. The important result is that daytime objects at ambient temperature show a spectral radiance minima around 3-4 μ.

The spectral distribution of terrain during the day may be represented by the solar scattering region occuring below 3μ with a peak around 0.5 μ, a minimum in the spectral radiance around 3-4 μ, and the thermal emission from terrain resulting in a peak in the spectral radiance near 10 μ. After sundown there is no longer interference from the sun due to scattering of its radiation in the region below 3 μ. The thermal radiation from the terrain follows changes in the terrain temperature, and the radiation from the 10 μ region is reduced after sundown.

The spectral transmission of the atmosphere must now be considered. The atmospheric windows were defined, and the absorption of radiation by water vapor and carbon dioxide was discussed. These atmospheric windows exist at 1.5-1.8 μ, 2.0-2.6 μ, 3.0-4.2 μ, 4.5-5.3 μ, and 8.0-14.0 μ. The most prominent absorption bands are the 2.7 μ region of both water vapor and carbon dioxide and the 4.3 μ carbon dioxide band.

The target to background contrast should be best between 3 μ and 5 μ . Glowing and burning fuels emit their maximum radiation near these limits and the background radiation from terrain has a spectral

radiance minimum around 3-4 μ . The atmospheric windows to be considered would be 2.0-2.6 μ , 3.0-4.2 μ, and 4.5-5.3 μ . The window at 8.0-14.0 μ could be used for fire detection, but thermal emission of terrain is present and detectors for this spectral region requires extensive cooling to temperatures less than 50°K. The effects of the solar scattering below 3 μ eliminates the window at 2.0-2.6 μ and also affects the window at 3.0-4.2 μ . Daytime operation favors the window at 4.5-5.3 μ with the window at 3.0-4.2 μ useable. For nighttime operation all three windows are useable. The spectral region for forest fire surveillance is the region from 3.0-6.0 μ .

Selection of the Infrared Detector

An infrared system for forest fire surveillance has as its primary function the detection of the target. The spectral region of operation is limited to the region from 3.0 to 6.0 μ . Infrared detectors having high D^* values over this spectral region are generally photoconductive or photovoltaic detectors. The high D^* values are usually obtained by cooling the responsive element. The proposed detection system is to be a field operating unit. Cooling the detector by liquid nitrogen is not easily accomplished in the field. Only those photoconductive or photovoltaic detectors capable of operation at 295 °K were considered.

Infrared detectors operation at 295 °K are given in Table II. The table lists only the detectors operating at 295 °K that possess the highest D^* values and also cover a portion of the spectral region from 3.0 to 6.0 μ . The detectors are the lead sulfide (PbS) detector, the lead selenide (PbSe) detector, and the indium arsenide (InAs) detector.

The PbSe detector was chosen as the detector having the best per-

TABLE II

INFRARED DETECTORS OPERATING AT 295 ^{o}K

Detector	Lead Sulfide PbS	Lead Selenide PbSe	Indium Arsenide InAs
Operational Mode	Photoconductive	Photoconductive	Photovoltaic
Wavelength Band	1 to 3.5 μ	1 to 5 μ	1 to 4 μ
$D^{*}(\lambda, m, f)$ (cm $(H_z)^{\frac{1}{2}}$/watt)	8×10^{10} f = 780	1×10^{9} f = 780	2×10^{9} f = 450
Time Constant (microsec)	100 to 500	≤ 2	≤ 2
Resistance per Square (ohm)	2 meg	≤ 10 meg	25
Cost	$49.00	$49.00	$175.00
Manufacturer	Santa Barbara Research Center	Santa Barbara Research Center	Texas Instruments

formance characteristics at 295°K because of its spectral response from 1-5 μ. The PbS detector for 295°K operation has a higher D* than either PbSe or InAs, but its spectral response is limited to 3.5 μ. The effects of the solar irradiance dominate the region below 3 μ. The PbS detector also has a larger time constant than the others. The InAs has a spectral response out to 4 μ, but it has a low impedance that requires the detector to be transformer coupled to the preamplifier. Transformer coupling is in general very sensitive to magnetic fields present when the detector must be placed next to chopper motors. A severe shielding problem may exist. Transformers used for this application are specially constructed; one such transformer is the Triad G-4 transformer. InAs does have the advantage that it does not require a bias circuit. Maximum detectivity of the InAs detector is achieved by cooling the detector to 196°K by use of a Peltier cooler. In the peak response region of InAs (3.3μ), the short time constants, and high detectivity of cooled InAs detectors offer decided advantages over cooled or uncooled PbS detectors. The cost of the InAs detector is considerably higher than PbSe. The PbSe detector was chosen because of its spectral response from 1-5 μ, its impedance is such that it can be coupled directly into a high impedance preamplifier, it has a relatively high D^*, it has a short time constant, and its cost is low.

System Components

This section describes the components actually used in the construction of the detection system. The system is illustrated by the block diagram shown in Figure 6. The incoming radiation is collected by the optical system and reflected onto the chopper which modulates

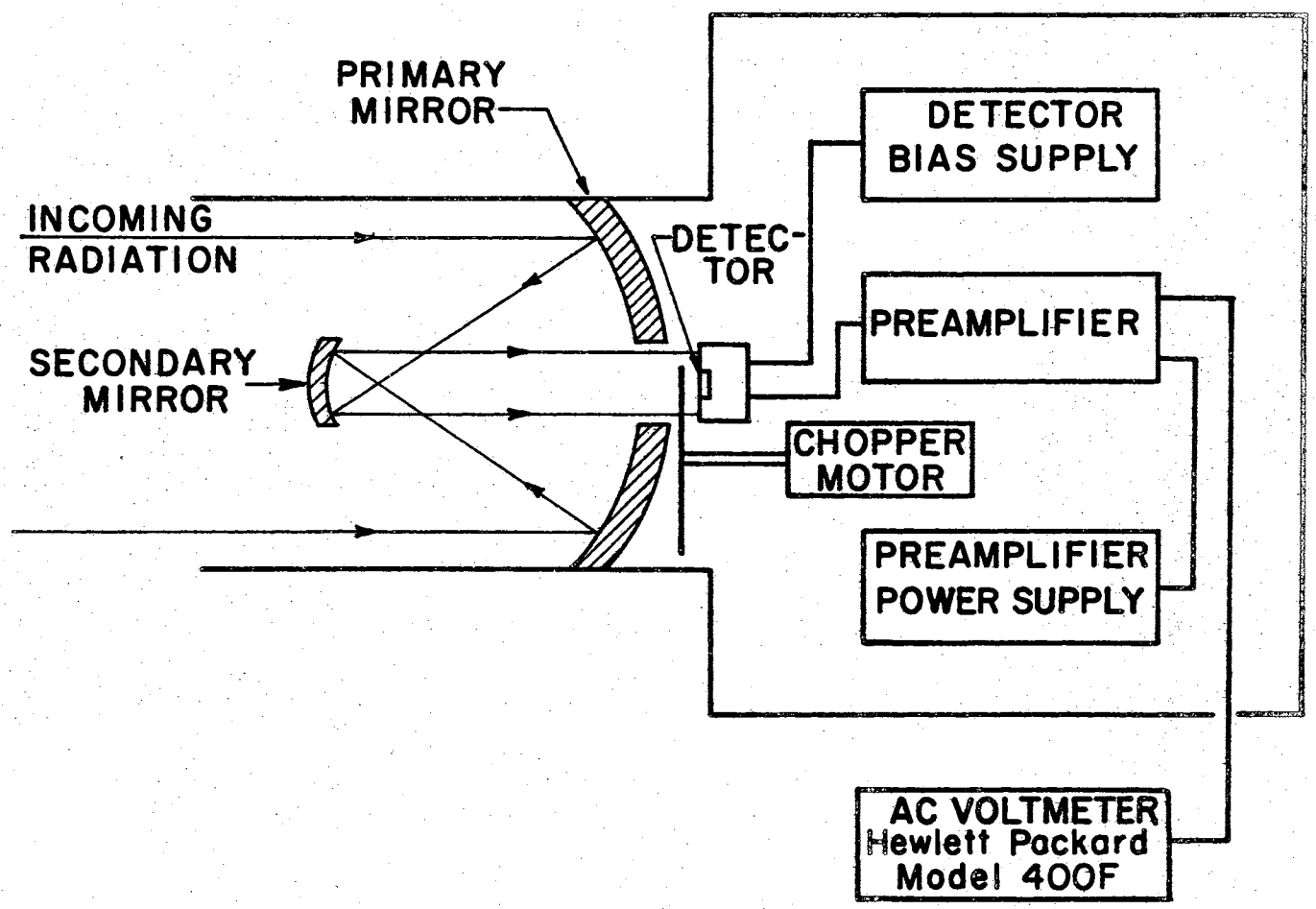

Figure 6. Block Diagram of Infrared System

the radiation falling on the detector. The fluctuating voltage from the detector's load resistor is placed across the input to the low noise preamplifier. The square wave output of the preamplifier is analyzed by an average responding rms ac voltmeter. A signal level is always present from background radiation while the system is in operation. Radiation from the target is detected when the ac voltmeter responds to a signal above the background radiation level. The spectral response curve for the PbSe detector is shown in Figure 7. Johnson, Cozine, and Mclean (20) have described the PbSe detector performance for 256°K to 373°K. The PbSe detector is a photoconductive detector and requires a bias voltage for its operation. A method for the determination of the optimum bias for a particular photoconductive detector is described by reference (11). The optimum bias E_b for a particular detector is usually supplied by the manufacturer (See Appendix A). The bias circuit for the PbSe detector is shown in Figure 8. The bias circuit consists of the 1 megohm load resistor R_1, the PbSe detector R_c and the bias battery. A change in the conductivity of the PbSe detector will be detected as a change in the voltage across the load resistor R_1 when the fixed bias E_b is applied across the detector R_c and the load resistor R_1.

The load resistor R_1 is a wire wound resistor or special low noise resistor which is selected to match the dark resistance of the detector. A mismatch between the detector impedance and the load impedance is tolerable. The load resistor used for the detector listed in Appendix A is a 1 megohm resistor. The dark resistance of the cell is 3 megohms. In order to permit use of an ac amplification system, the radiation falling on the PbSe detector is modulated by means of a chopper blade

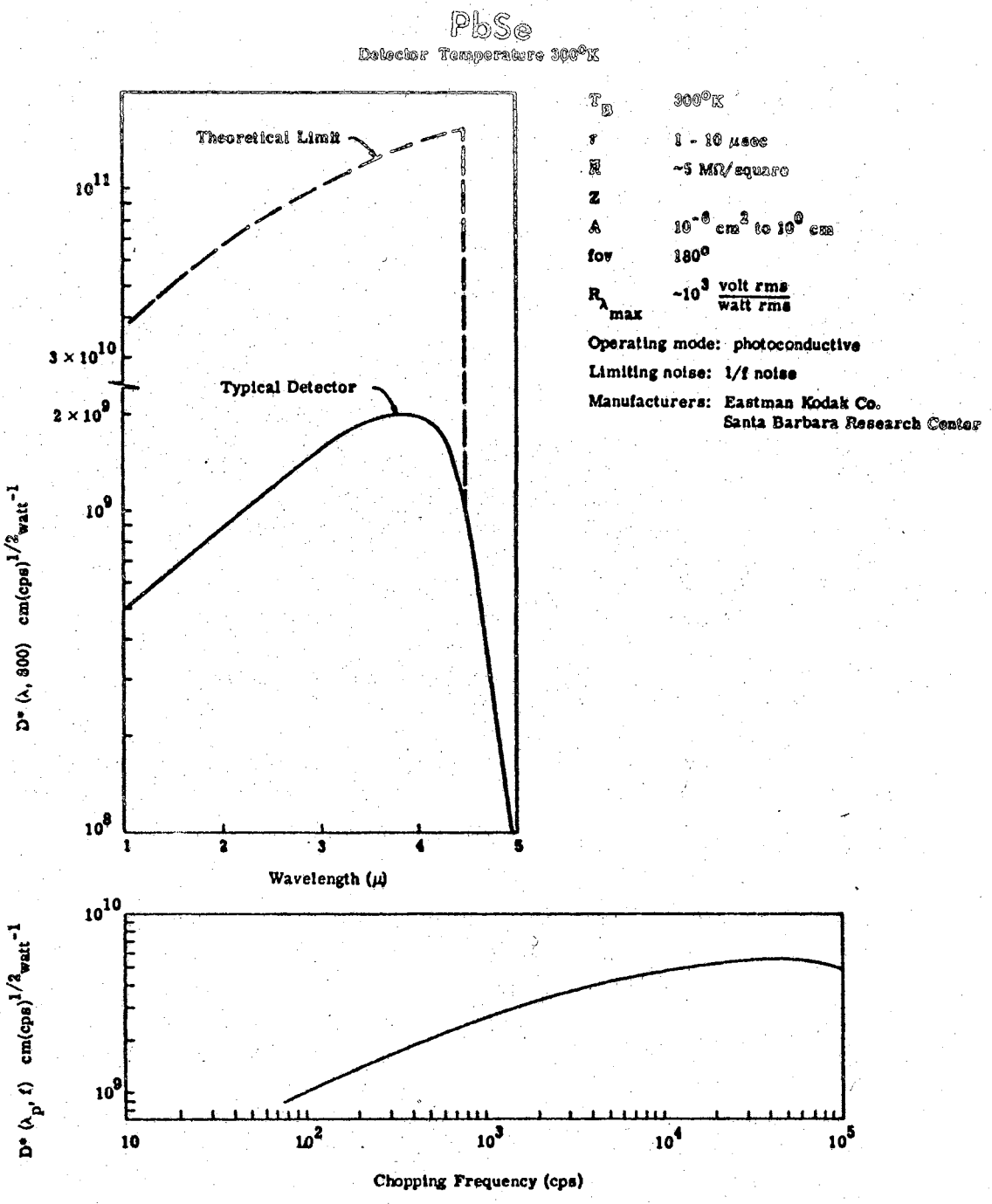

Figure 7. Spectral Response Curve for PbSe Detector (After Reference 11).

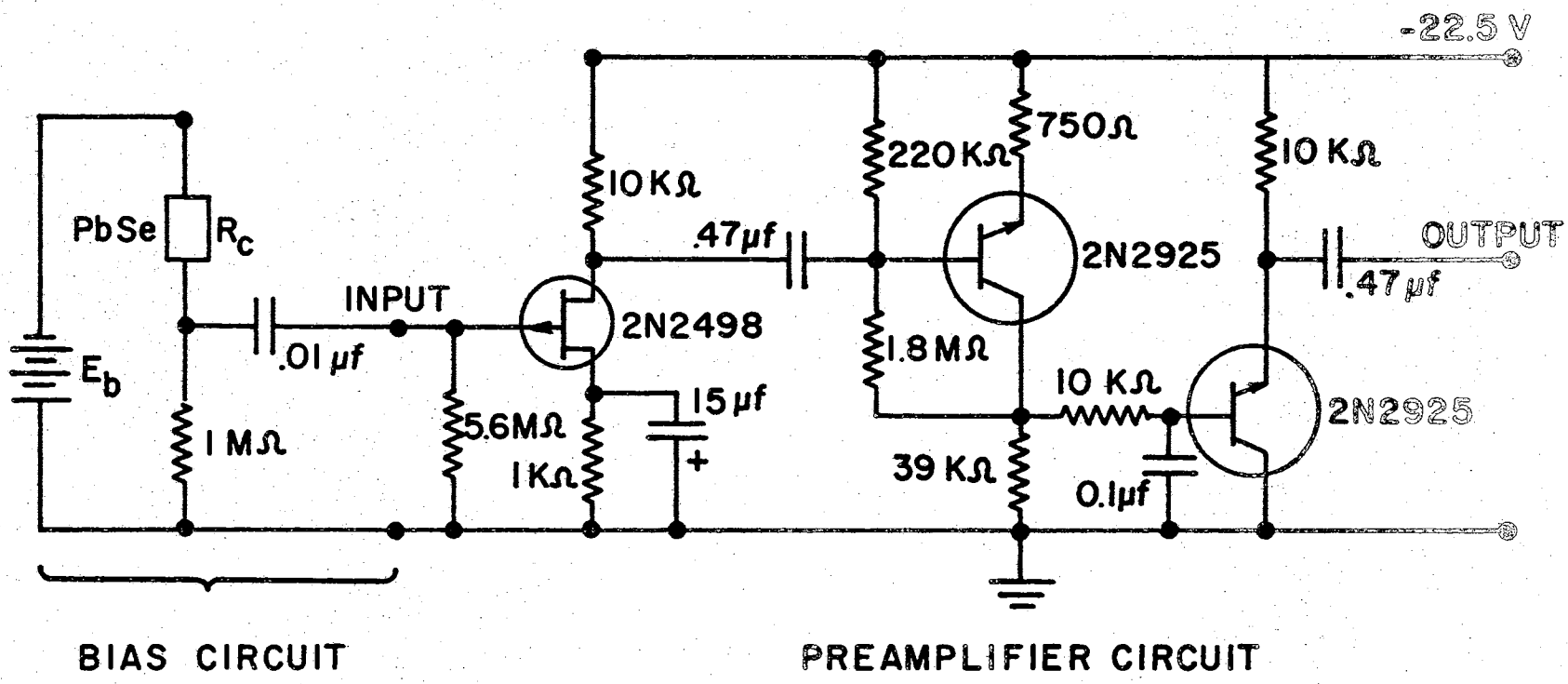

Figure 8. Detector Bias Circuit and Preamplifier Circuit

to produce a fluctuating voltage signal whose amplitude is related to the intensity of the incident radiation.

The PbSe detector is mounted in a shielded enclosure and the chopper is placed immediately in front to modulate the incident radiation.

The PbSe detector responsive element is a film chemically deposited upon a quartz substrate. The detector parameters for the particular PbSe detector used in the detection system are listed on the detector data sheet given in Appendix A. It is a 2mm x 2mm detector operating at 295°K. The D^* values have been measured at an optimum chopping frequency of 840 H_z. The chopper motor used in the detector system uses a ten blade chopper to chop the incoming radiation at 900 H_z. The chopper motor operates from a 12 v battery and draws 0.18 amp. The PbSe detector and its bias circuit have been described. The optimum bias voltage E_b for the detector is 100 v and is supplied by a bias battery. The current in the bias circuit is 25 microamp. The dark resistance of the detector is 3.0 megohms.

The preamplifier used in the detection system is a low noise, high input impedance amplifier. The amplifier uses a field effect transistor (FET) for the input stage. The term "noise figure" is used to describe the noisiness of a device. The 2N2498 FET transistor is capable of a low noise figure of less than 3db. The FET provides the low noise figure in the low-frequency region (less than 10KH_z), and allows low noise designs for source impedances into the megohm region. The circuit diagram of the preamplifier built for the detection system is shown in Figure 8. The amplifier has a fixed gain of 100 and an input impedance of 10 megohms. The power supply is a 22½ volt battery and the current drain is 2 milliamps. The preamplifier must take the detector signal

level in the order of microvolts (See Appendix A for Signal Level) and transmit this signal over a cable to the ac voltmeter. The primary objective is to produce a preamplifier that matches the impedance of the detector and has a lower noise level than the detector. The noise level of the detector is then the primary source of noise in the system.

Construction of the system demanded that all electronic components be carefully shielded to prevent the introduction of noise into the detector signal by stray fields. The preamplifier, the detector and the detector bias supply all required shielding. Shielded cable was used for all connections between the various components of the system. The detector bias circuit is shown in Figure 8. Other components can be seen in Figure 9.

The preliminary appraisal of mirror systems for use in a fire detection system considered reflecting optical systems. Such a system could be a simple spherical mirror or a compound reflecting optical system (Figure 6). The focal point of a spherical mirror lies in front of the mirror's reflecting surface. The photodetectors that were considered generally require that the incident radiation be modulated by a chopper. It is difficult at best to locate the photodetector and chopper motor at the focal point of a spherical mirror. A compound reflecting system or folded system locates the focal point of the mirror system behind the primary mirror. In this case, the photodetector and chopper motor can be conveniently located behind the primary mirror.

Two folded systems were of interest, the Cassegrainian system, and the Gregorian telescope. The Cassegrainian system uses a parabolic reflector for its primary mirror and a hyperbolic reflector for its secondary mirror. The Gregorian telescope consists of a parabolic pri-

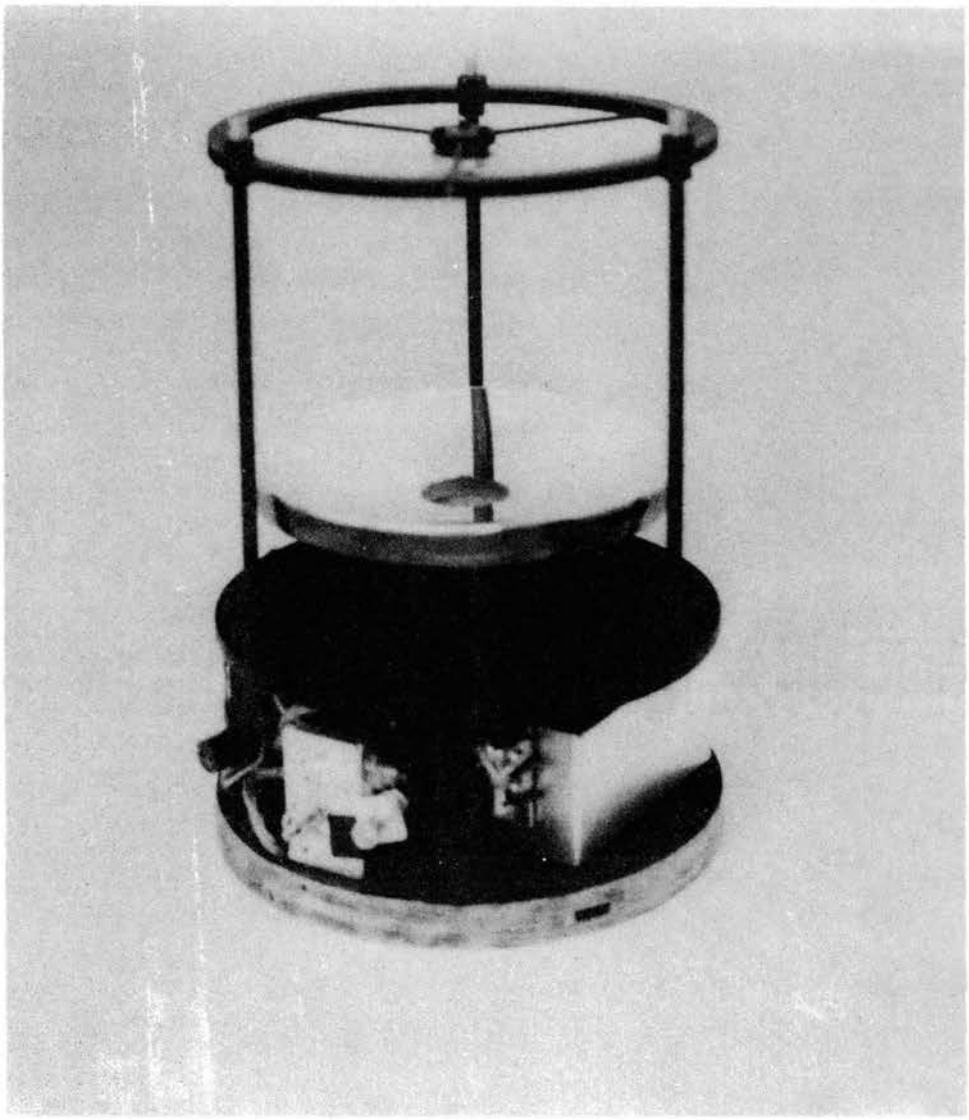

Figure 9. Infrared System Assembly

mary mirror and an elliptical secondary mirror. Mirrors for infrared instrumentation are generally not commercially available but are custom designed for each particular application. Investigation as to the cost of such systems placed the starting price at $1500. This type of system was thus beyond the budget of the project.

The optical system used in the infrared detection system is pictured in Figure 9, and in Figure 6 the system is shown schematically. The optical system consists of a 6½" spherical primary mirror and a 1 1/8" spherical secondary mirror. The primary mirror has a focal length of 4" and the secondary mirror has a focal length of 5/8". The first-surface mirrors have a high-reflecting coating of vacuum-deposited aluminum. Durable, thin evaporated aluminum coatings have a reflectance of more than 95% between 2 and 10 μ (11).

The mirrors used in the optical system are arranged to form an afocal system. An afocal system has its object and image at infinity and thus has no focal length. An afocal system composed of two components is so arranged that the image of the first component, which is the object for the second, lies exactly at the first focal point of the second component and is thus reimaged at infinity. The incoming radiation is not focused onto the detector. The optical system was used because it was on hand in the laboratory. It was realized that it would be far from ideal.

The completed infrared detection system is shown mounted on a tripod in Figure 10. The detection system is housed in a plastic cylinder. The interior of the cylinder was sprayed with flat black paint to minimize reflections inside the system. The ac voltmeter is also shown in the picture with its own power supply. The other battery is the 12 volt

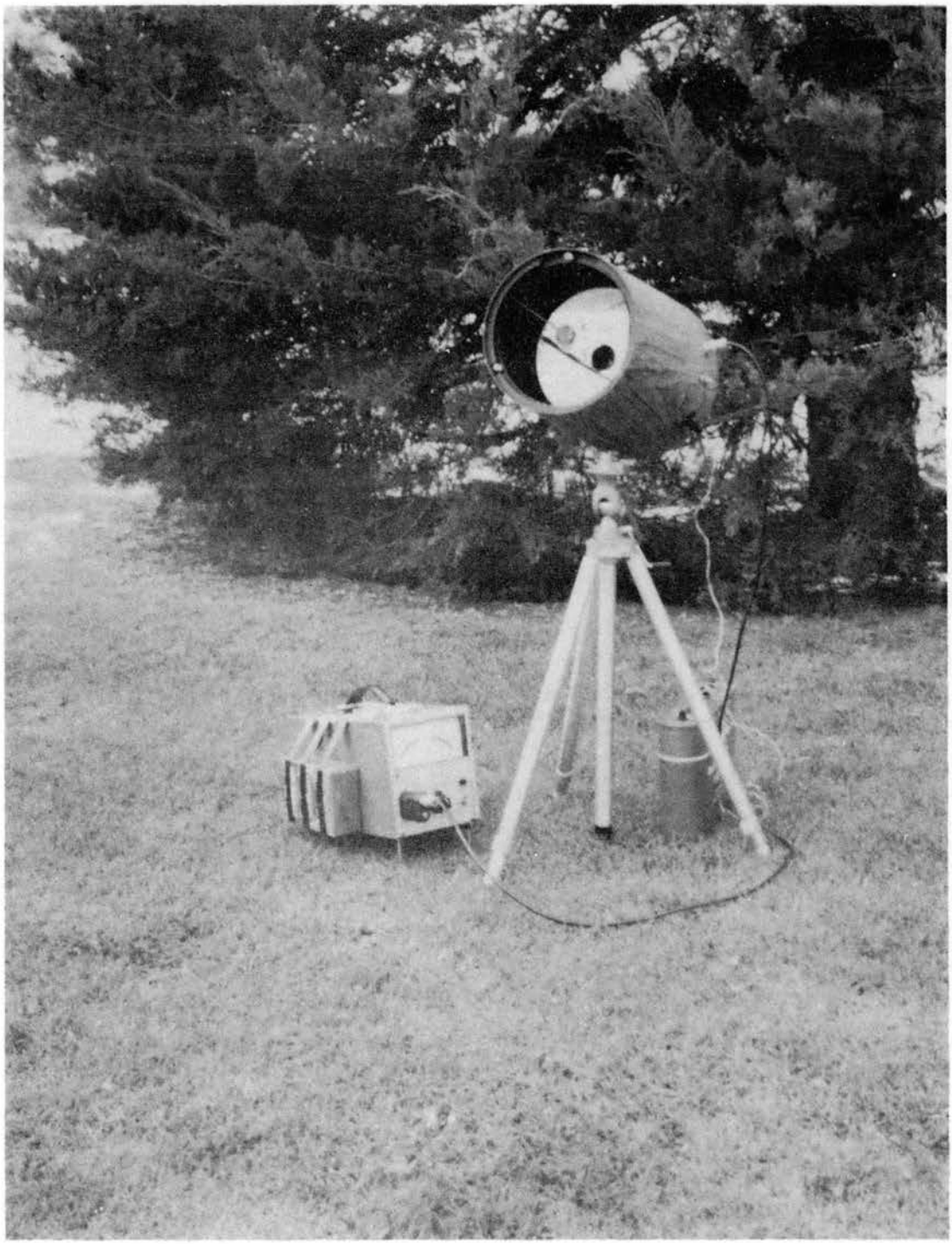

Figure 10. Picture of Operational Infrared System

supply for the chopper motor.

CHAPTER IV

SUMMARY AND CONCLUSIONS

The primary objective of this thesis was to design and construct an infrared system to detect incipient forest fires. The infrared system was field tested using a small fire as a target. Target to background measurements were made during the day and during the night. From the field test was gained an appreciation for the discrimination of a target against various backgrounds. Background radiation possesses a difficult discrimination problem for infrared equipment. The primary objective was to investigate the various parameters and problems of fire detection and not necessarily optimize the performance of the infrared system constructed.

The target used in the field test consisted of five logs, 4" in diameter and 2 feet long, stacked to form a small fire. The target was observed in daylight shortly before sundown while the effects of solar interference could be observed, and the target was observed at night when the background radiation would be due primarily to the terrain. The target was observed at various distances by the infrared system, and the results of the field test are presented in Table III.

The effects of solar radiation were easily observed during the daylight operation of the system. At 30 feet from the target when the target fills the field of view of the system, the target was easily discriminated against the background, and the effect of solar interference

TABLE III

FIELD TEST DATA

Daylight Observation			
Location of System	Target	Terrain Background	Sky Background
30 ft. Shade	0.70 v	0.25 v	0.45 v
70 ft. Shade	0.60 v	0.20 v	0.50 v
100 ft. Direct Sun	0.60 v	0.50 v	0.50 v
Night Observation			
Location of System	Target	Terrain Background	Sky Background
30 ft.	0.70 v	30 mv	35 mv
70 ft.	0.25 v	30 mv	
150 ft.	37 mv	24 mv	
200 ft.	26 mv	17 mv	
225 ft.	25 mv	15 mv	
250 ft.	28 mv	25 mv	

was not observed. When the detection system was at 100 feet the effect of the solar radiation was readily observed. The sky background is primarily caused by the scattering and the reflection of solar radiation by the atmosphere and particles in the atmosphere. The signal level of the sky background was 0.5 volts. With the detection system located in the shade, the background signal level of the terrain was 0.2 volts. When the detection system was located in direct sunlight the signal level was 0.5 volts. Thus, when the system is located in direct sunlight, the effects of solar interference predominate the radiation from the terrain. Most of the radiation from the target occurs in the 3μ to 6μ region, but the problem of discriminating the target from daylight background radiation and its fluctuations is a serious one for the infrared detection system. The background radiation can be greatly reduced by optically filtering out all received radiation below 3μ. The effect of the optical filters on the radiation flux entering the system is taken into account by the transmission factor τ_o which was discussed earlier.

Night observation of the target resulted in increased range in the detection system. At night the background radiation that was due to solar radiation during the day is no longer present. Only the background radiation due to the thermal emission of the atmosphere and terrain is present. The signal level of the night background was about 25 millivolts. A lower background radiation level than was present for daytime observation results in a better signal to noise ratio and a corresponding increase in the range of the system.

The night the field test was conducted the sky was clear and a quarter-moon was present. The radiant energy received from the moon is

solar radiation that has been modified by reflection from the lunar surface and absorption by the intervening atmospheres. The effect of moonlight was noted by observing the moonlight reflected from the trees. The background level from the moonlit trees was 35 millivolts. The background level from the other background was 25 millivolts. The sky background in this instance is now due primarily to scattered moonlight. The sky background signal level was 35 millivolts. Moonlight introduces another source of background radiation which the target must be discriminated against.

This simple system does provide an understanding of the forest fire detection problem. Field test results provided an appreciation for the discrimination of the target against terrain and sky backgrounds. The design phase provided experience on equipment design and component layout. The problems experienced during construction were problems of shielding and component placement.

The performance of this system could be greatly improved by incorporating into it one of the other folded optical systems discussed previously. The optical system used was far from ideal. The other components, the detector, and the preamplifier were carefully selected, and the results that were obtained were due to these selections.

BIBLIOGRAPHY

1. E. Scott Barr, "Historical Survey of the Early Development of the Infrared Spectral Region," Am. J. Phys. 28, 42 (1960).

2. R. A. Smith, F. E. Jones, and R. P. Chasmar, The Detection and Measurement of Infrared Radiation, (Oxford University Press, New York, 1957).

3. "Special Issue on Infrared Physics and Technology," Proc. I.R.E. (Inst. Radio Engrs.) 47, (1959).

4. "The Infrared Issue," J. Appl. Opt. 1, (1962).

5. S. N. Hirsch, "Possible Application of Electronic Devices to Forest Fire Detection," U.S. Forest Serv., Intermountain Forest and Range Exp. Sta., Res. Note No. 91, (1962).

6. S. N. Hirsch, "Applications of Remote Sensing to Forest Fire Detection and Suppression," Univ. of Mich. Inst. of Sci. and Technol., The Second Symposium on Remote Sensing of Environ. Proc., 295 (1962).

7. R. A. Wilson and Nonan V. Noste, "Project Fire Scan Fire Detection Interim Report," April 1962 to Dec. 1964, U.S. Forest Serv., Intermountain Forest and Range Exp. Sta., Res. Paper INT-25, (1966).

8. R. A. Wilson, "The Remote Surveillance of Forest Fires," J. Appl. Optics 5, 899 (1966).

9. P. W. Kruse, L. D. McGlauchlin, and R. B. McQuistan, Elements of Infrared Technology, (John Wiley and Sons, Inc., New York, 1962).

10. J. A. Jamieson, R. H. McFee, G. N. Plass, R. H. Grube, and R. G. Richards, Infrared Physics and Engineering, (McGraw-Hill Book Company, Inc., New York, 1963).

11. Handbook of Military Infrared Technology, Ed. W. L. Wolfe, (Office of Naval Research, Department of the Navy, Washington, D.C., 1965).

12. M. R. Holter, S. Nudelman, G. H. Suits, W. L. Wolfe, and G. J. Zissis, Fundamentals of Infrared Technology, (The Macmillan Company, New York, 1962).

BIBLIOGRAPHY (Continued)

13. H. L. Hackforth, Infrared Radiation, (McGraw-Hill Book Company, Inc., New York, 1960).

14. N. Dittmar, F. Farley, and J. Boyse, "Earth Background Measurements: A Survey of the Unclassified Literature," The University of Michigan, Willow Run Labs., Inst. of Science and Technology, Rept. No. 6054-16-X.

15. H. W. Yates and J. H. Taylor, "Infrared Transmission of the Atmosphere," NRL Report 5453, U.S. Naval Research Laboratory, Washington, D.C. (1960) ASTIA AD240188.

16. R. C. Jones, D. Goodwin, and G. Pullan, "Standard Procedure for Testing Infrared Detectors and for Describing Their Performance," Office of Director of Defense Research and Engineering, Washington, D.C. (Sept. 1960).

17. L. Larmore, "Range Equation for Passive-Infrared Devices," Proc. of the IRE 47, No. 9, 1489 (1959).

18. K. Knight, "Range Equation for Active Devices," Proc. of the IRE 47, No. 9, 1490 (1959).

19. N. C. Stirling, "Detection Range Prediction for Infrared Detection Systems," Proc. of the IEEE 51, No. 10, 1327 (1963).

20. T. H. Johnson, H. T. Cosine, and B. N. Mclean, "Lead Selenide Detectors for Ambient Temperature Operation," J. Appl. Opt. 4, 693 (1965).

APPENDIX A

DATA SHEET FOR PbSe DETECTOR

SANTA BARBARA RESEARCH CENTER

A Subsidiary of Hughes Aircraft Company

75 COROMAR DRIVE • GOLETA, CALIFORNIA

TELEPHONE: 968-3511

14 March 1968

W/A 5298
P.O. No. 05449

OKLAHOMA STATE UNIVERSITY
Stillwater
Oklahoma

Re: PbSe Style 10A IR Detector, 2 mm x 2 mm
Element Size

TEST CONDITIONS

Blackbody Temperature:	$500^{\circ}K$
Blackbody Flux Density:	8.05×10^{-6} watt/cm^2
Chopping Frequency:	840 Hz
Noise Bandwidth:	15 Hz
Bias Voltage:	100 volts
Load Resistance:	1.0 megohm
Detector Temperature:	$295^{\circ}K$

TEST RESULTS

Detector No.	Impedance (megohms)	RMS Noise (μV)	Signal (μV)	D*($500^{\circ}K$, 840) cm Hz$^{\frac{1}{2}}$/watt	CALCULATED D*(λ_m, 840) cm Hz$^{\frac{1}{2}}$/watt	Blackbody Responsivity (volt/watt)
5298-1	3.0	1.7	290	4.1×10^8	4.1×10^9	9.0×10^2

VITA

Ronald Keith Jantz

Candidate for the Degree of

Master of Science

Thesis: DESIGN AND CONSTRUCTION OF AN INFRARED DETECTION SYSTEM FOR FOREST FIRES

Major Field: Physics

Biographical:

Personal Data: Born in Hillsboro, Kansas, July 30, 1938, the son of Frank and Edna L. Jantz. Married Janice K. Funk on August 26, 1961.

Education: Graduated from East High School, Wichita, Kansas, in May 1956; received the Bachelor of Science degree from University of Wichita, with a major in Physics, in June, 1961; completed requirements for the Master of Science degree from Oklahoma State University, with a major in Physics, in May, 1969.

Professional Experience: Teaching Assistant in Physics Department, Oklahoma State University; Physicist with Harry Diamond Laboratories, Washington, D.C., from 1965 to the present.

Organizations: Member of Sigma Pi Sigma.